15 Scale Testing

P. D. Allen

CONTENTS

I. INTRODUCTION

The use of roller rigs for the investigation of railway vehicle dynamics has been discussed in Chapter 14. Their operation, application, and the changes in vehicle response introduced due to geometric and kinematic differences between running a rail vehicle on rollers, as opposed to track, were described in detail. Full scale rigs are a useful tool when assessing the dynamic performance of a prototype vehicle, especially in the days when numerical simulation of vehicle dynamics was not as well developed as it is today, but their frequency of use for prototype design is in decline, as computer techniques become more popular. Their high costs act against their widespread use.

Where the area of research is rather broader, and the behaviour of a particular prototype vehicle is not the primary area of interest, then the use of a scaled roller rig can offer a number of advantages. The most obvious of these advantages is, of course, the space occupied by the rig, this is coupled to a large cost saving and an ease of operability. A scaled rig is much easier to maintain and the mechanical handling of the test vehicle is more manageable. It is also far easier to change

a large number of vehicle parameters without great effort. However, these advantages must be offset by a number of negative factors. These are primarily concerned with the effect of scaling down the vehicle dimensions. From a scientific viewpoint, it is not acceptable to reduce the dimensions of the vehicle without giving due consideration to the effect of these changes. It is of great importance, if reliable scaled results are to be obtained, to adopt a scientifically based scaling strategy. The outcome of this strategy will dictate how well the rig will relate to the full scale, whether this is in terms of vehicle dynamics, wheel–rail forces or even wear.

This chapter describes a number of scaled roller rigs, used as research tools, and how each of the institutions involved have handled the issues related to scaling. Examples are given of the errors which can be introduced by different types of scaling strategies.

The fundamental ideas of similarity, that is, maintaining correlation between a scale model and the full scale, can be traced back to the work of Reynolds,[1,2] or even earlier. Analogous to Reynolds approach, similarity of mechanical systems with respect to dynamic behaviour and elastic deformation can be defined.

Small-scale testing of railway vehicles on roller rigs has been carried out for different purposes, including the verification and validation of simulation models, the investigation of fundamental railway vehicle running behaviour (nonlinear response, limit cycles, etc.), for the development and testing of prototype bogie designs with novel suspensions, in order to support field tests and computer simulations and last but not least for teaching and demonstration of railway vehicle behaviour. Small-scale tests at various institutions have proven that under laboratory conditions, influences of parameters can be revealed which often cannot be separated from stochastically affected measurements of field tests, which is of course also true for full scale rigs.

II. A BRIEF HISTORY OF SCALED ROLLER RIGS

Investigations using scaled models of railway vehicles on scaled tracks were performed by Sweet et al.[3,4] at Princeton University in 1979 and 1982. Experiments were concerned with the mechanics of derailment of dynamically scaled 1/5 model of a typical three-piece freight truck design widely used in North America. Careful attention was given to the scaling of clearances. Forces were scaled according to similarity laws, including the effects of inertia, gravitation, spring stiffness, creep, and dry friction. These methods have been adopted and are used in many of the currently adopted scaling strategies.

One of the first investigations in Germany on a scaled roller rig was performed by the RWTH Aachen.[5] Other designs of scaled roller rigs followed, in 1984 at DLR Oberpfaffenhofen,[6–8] in 1985 at the Institut National de Recherche sur les Transports et leur Securite (INRETS) in Arcueil,[9] and in 1992 at the Rail Technology Unit of the Manchester Metropolitan University (MMU).[10–12]

III. SURVEY OF CURRENT SCALED ROLLER RIGS

There are a number of scaled roller rigs which are used for research and demonstration purposes. The design and operation of some of the scaled roller rigs in use today are described in the following section.

A. The Scaled Rig of DLR

The Institute for Robotics and System Dynamics of DLR has been involved in the development of simulation software for railway vehicle dynamics based upon multibody modelling techniques since the early 1970s.

The institute was interested in the nonlinear running behaviour of railway passenger vehicles and experiments became very important for the validation of modelling work which was carried out to predict the dynamic response of the vehicle. In wheel–rail dynamics, the nonlinear forces

involved play a dominant role in the onset of vehicle hunting, a phenomenon which is caused by a bifurcation of the system's equations of motion into a periodic solution or limit cycle as it is commonly referred to. For this reason, DLR developed a scaled roller rig, with a single bogie vehicle running on the rollers. The primary functions of the rig were to perform the above validation but also to assist in the verification of parts of DLR's dynamic simulation software, SIMPACK.

The bogie was a scaled-down version of the MAN bogie.[6,7] The emphasis of the first series of tests were the fundamentals of modelling and experimental methods in wheel–rail dynamics. Once this first stage of work was completed, including investigations of limit cycle behaviour of the bogie,[8] DLR adapted the rig to concentrate on the development of unconventional wheelset concepts, and contributed to fundamental research in this field.[13]

1. Design Overview

The roller rig at DLR is a 1/5 scale rig consisting of two rollers, each of which is composed of a hollow cylinder, with a wall thickness of about 20 mm. At each end of the cylinder a disc is attached, which has formed around its circumference a 1/5 scale UIC60 rail profile. The diameter of this part of the roller is 360 mm and the separation of the disc is 287 mm, which is 1/5 of the standard track gauge of 1435 mm. The advantage of this type of roller construction is that the design provides a very high torsional stiffness, which is important in maintaining a true creepage relationship between the wheel and roller. This stiffness coupled with a large rotational inertia, which makes the rollers insensitive to disturbances of their rotational velocity, makes the arrangement well suited to simulating tangent track behaviour. A plan view drawing of the rig is shown in Figure 15.1.

The distance between the rollers can be varied to accommodate different bogies with different wheelbase. A feature of this arrangement is the inclusion of a "Schmidt-Coupling," this device is a parallel crank mechanism and allows the change of wheelbase without disruption to the drive arrangement. As can be seen in the sectional view, the rollers are mounted on cones, this allows easy removal of the rollers for changes to rail profile or gauge.

The rollers are interconnected using a toothed belt with a specified longitudinal stiffness to maintain the synchronisation of the roller speeds at all times. The roller speed can be varied from 0 up to 168 km/h, depending on the rolling resistance of the vehicle being modelled. The general arrangement, showing a MAN bogie being tested on the rig is shown in Figure 15.2.

B. The Scaled Rig of MMU

A 1/5 scale roller rig was set up at Manchester Metropolitan University (MMU) in 1992 for use in the investigation of railway vehicle dynamic behaviour and to assist in research, consultancy, and teaching activities. Research activities then focused on the evaluation of a novel design of differentially rotating wheelset and the quantification of errors inherent in roller rig testing.[12] The roller rig is currently being used to investigate the behaviour of independently driven wheelsets for light rail applications.

1. Design Overview

The roller rig at Manchester Metropolitan University is of 1/5 scale, and consists of four rollers supported in yoke plates incorporating the rollers supporting bearings, with the interconnection between the roller pairs being provided by the use of splined and hook jointed shafts. While these shafts do not offer the degree of torsional stiffness given by the DLR arrangement, they do allow the simulation of lateral track irregularities by enabling rotational movement of the rollers about a vertical axis (yaw), coupled with a lateral movement of the rollers as a pair. The roller motion is provided by servo hydraulic actuators which are connected directly to the rollers supporting yoke plates, these actuators being controlled by a digital controller which allows the inputs to follow

defined waveforms or measured track data. The longitudinal and lateral position of the rollers can be adjusted by means of a system of linear bearings for changing the wheelbase and the gauging of the rollers. Drive is supplied to the rollers via a belt, with pulleys on each roller drive shaft, allowing the rig to operate at scaled speeds of up to 400 km/h. The bogie is modelled on the BR Mk IV passenger bogie,[14] but it can be easily modified. The purpose of the rig was to demonstrate the behaviour of a bogie vehicle under various running conditions and acquire nominal data from the vehicle responses. A plan view drawing of the roller rig is shown in Figure 15.3.

The bogie vehicle parameters were selected to represent those of a typical high speed passenger coach (the BR Mk4 passenger coach). The wheel profiles are machined scaled versions of BR P8 profile and the rollers have a scale BS110 rail profile with no rail inclination. The bogie running on the rig can be seen in Figure 15.4.

C. The Scaled Rig of INRETS

INRETS is the French national research institute and within this is a group specialising in wheel–rail interaction, with particular interest in the novel variations of freight bogies. The test facility was originally commissioned in 1984 and was used intensively until 1992.

The first railway vehicle to be tested on the rig was the Y25 type, a UIC bogie,[15] which is very common in Europe. The bogie was selected as it is particularly difficult to model with conventional

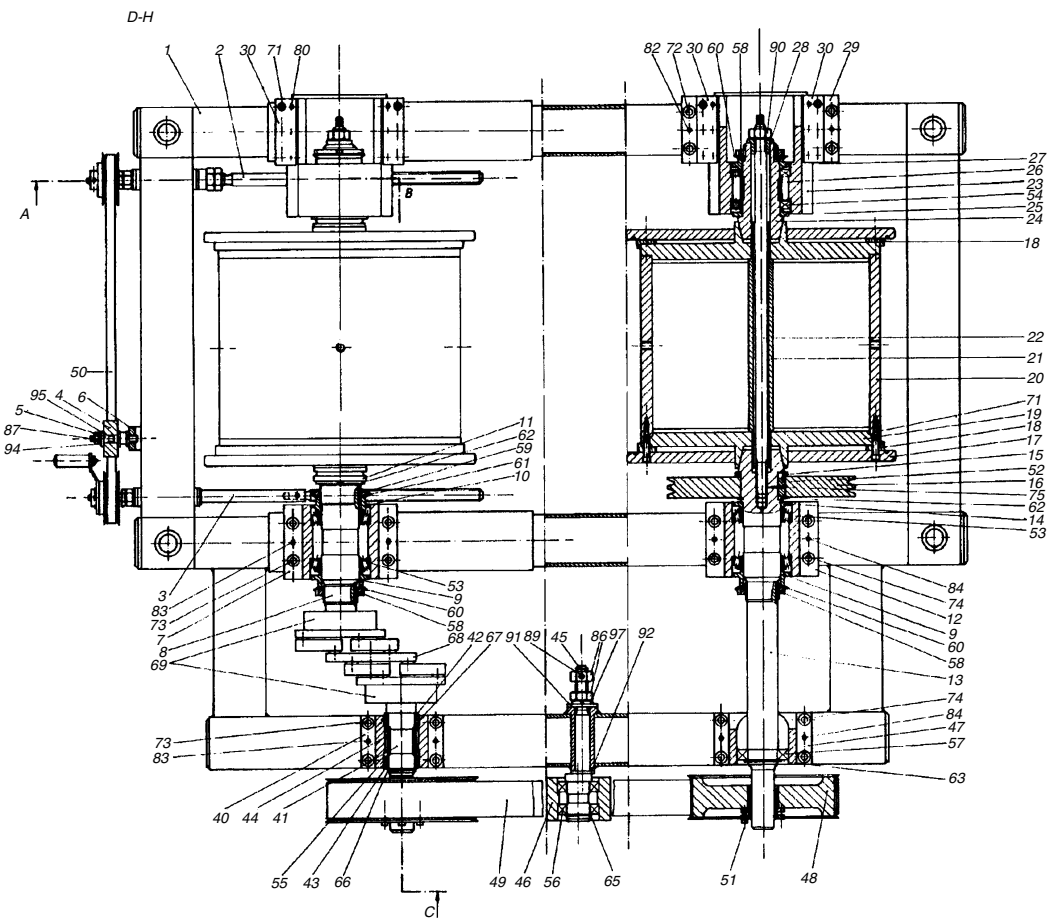

FIGURE 15.1 Plan view drawing of the 1/5 scale DLR roller rig.

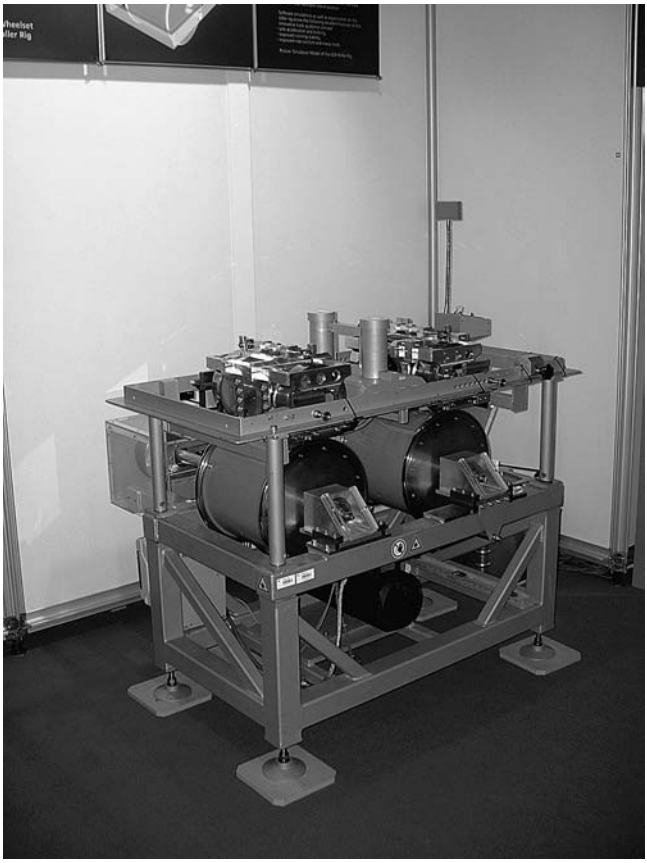

FIGURE 15.2 The MAN bogie model under test at DLR.

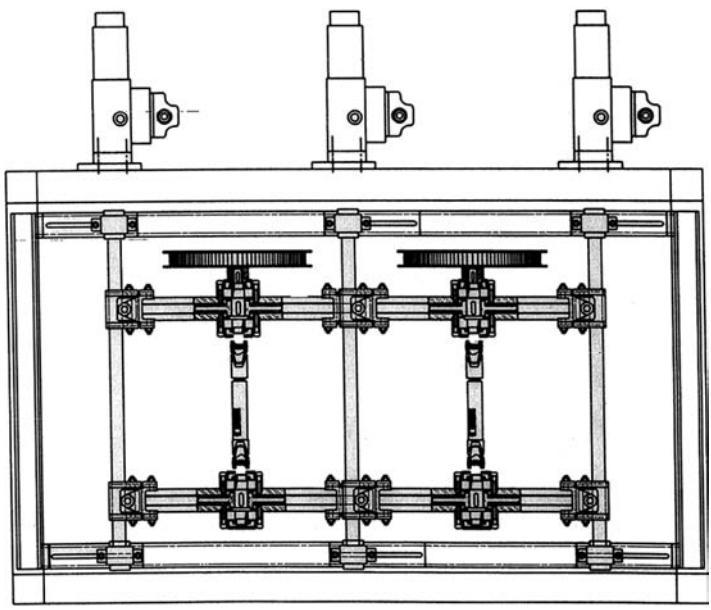

FIGURE 15.3 Plan view drawing of the roller rig at MMU.

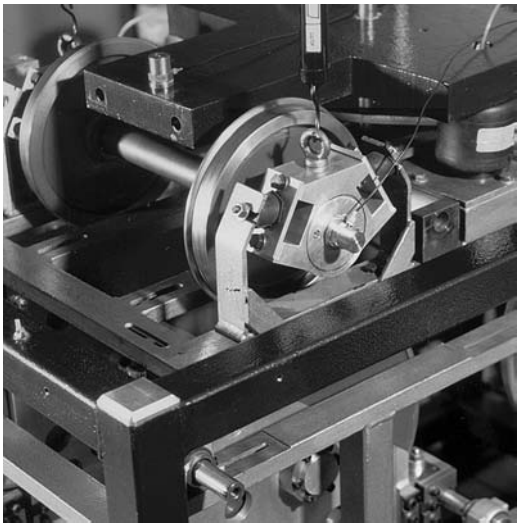

FIGURE 15.4 Bogie vehicle on the MMU roller rig platform.

computer software as there are several dry friction dampers within the suspension. Studies focused on optimising the stability of the bogie under varying vertical loads and differing suspension parameters.

Latterly the rig has been used for the quasistatic measurement of the Kalker coefficients and currently experiments are being carried out dealing with squeal noise and braking performance.

1. Design Overview

The test rig of the Institut National de Recherche sur les Transports et leur Securité (INRETS) was originally designed as a large flywheel of 13 m diameter to test linear motors for the Bertin Aerotrain transport vehicle and this is the reason the wheel is of such large diameter. Weighing 40 t, the wheel is driven by a linear 2 MW motor, which can power the wheel to a periphery speed of 250 km/h.

The flywheel was not designed to support very high vertical loads and therefore a scaling factor of 1/4 was chosen for the rig. INRETS were already familiar with similarity laws used in scale models, and developed a specific strategy for dynamic similarity, with respect to the preservation of the elasticity of the bodies, especially for the wheel–rail contact area. The rig is illustrated in Figure 15.5.

The large diameter of the test wheel made the rig at INRETS particularly suitable for investigating the contact between wheel and rail as the radius of curvature was far closer to approaching that of conventional track, when compared to any other roller rig in existence, resulting in the size and shape of the contact patch being closer to reality.

The wheel can only rotate about the horizontal axis, and therefore an angle of attack can only be generated by yawing the vehicle wheelset relative to the track. A hydraulic ram is fitted at the top of the wheel to allow the variation of the vertical load on the tested bogie.

IV. ROLLER RIGS: THE SCALING PROBLEM

Similarity laws and the correlated problem of scaling are of interest for the transformation of experimental results from a scaled model to the full scale design. There are various possible

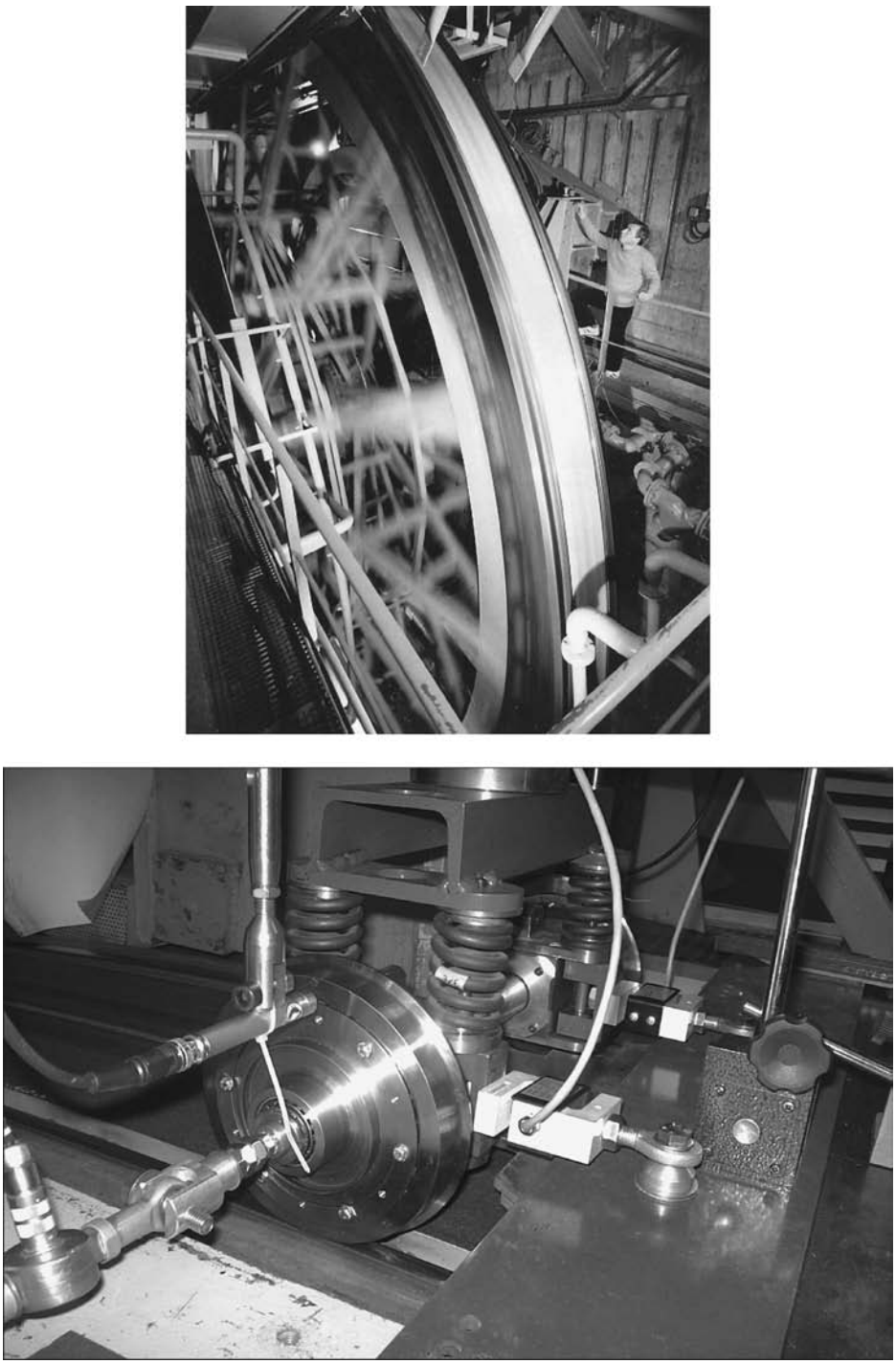

FIGURE 15.5 The INRETS rig at Grenoble.

approaches to scaling, including using the methods of dimensional analysis to establish several dimensionless groups from which the scaling factors can be derived, workers include, Jaschinski,[8] Illingworth,[21] and Chollet.[15] Other methods include first deriving the equations of motion and then calculating the scaling factors required for each term to maintain similarity.

This latter method is known as inspectional analysis and requires a sound understanding of the equations of motion, which is achievable in this particular field.

Choice of material properties is also a factor in the scaling method used, particularly if the simulation work requires the preservation of the levels of strain at the contact point. British Rail used aluminum wheels and rollers,[18] while Matsudaira et al.,[19] used steel, and Sweet et al.[3] used plastic.

The starting point for defining a system of similarity is the definition of the length scaling factor and defining the general terms. These general terms are outlined below, it is from these that the scaling strategies of the three research institutions are developed.

$$\varphi_l = \frac{l_1}{l_0} \tag{15.1}$$

where l_1 is a characteristic length of the full scale and l_0 that of the scaled model. In the same way, a time scaling factor can be derived.

$$\varphi_t = \frac{t_1}{t_0} \tag{15.2}$$

With these definitions, scaling factors for cross-section, φ_A, volumina, φ_V, velocity, φ_v, and acceleration, φ_a, follow:

$$\varphi_A = \varphi_l^2 \tag{15.3}$$

$$\varphi_V = \varphi_l^3 \tag{15.4}$$

$$\varphi_v = \frac{\varphi_l}{\varphi_t} \tag{15.5}$$

$$\varphi_a = \frac{\varphi_l}{\varphi_t^2} \tag{15.6}$$

When the density scaling φ_ρ is

$$\varphi_\rho = \frac{\rho_1}{\rho_0} \tag{15.7}$$

then the scaling factors for mass, φ_m, moment of inertia, φ_I, and inertial force, φ_F, can be derived:

$$\varphi_m = \varphi_\rho \varphi_l^3 \tag{15.8}$$

$$\varphi_I = \varphi_m \varphi_l^2 \tag{15.9}$$

$$\varphi_F = \frac{m_1 a_1}{m_0 a_0} = \varphi_m \varphi_a = \frac{\varphi_\rho \varphi_l^4}{\varphi_t^2} \tag{15.10}$$

Once these general definitions have been developed, the scaling strategies of each institution can be used to derive the following quantities used in studies of wheel–rail interaction: φ_T, scaling factor for creep forces; φ_{ab}, scaling factor for the elliptical size of the contact patch; φ_E, scaling

factor for Young's modulus; φ_ν, scaling factor for Poisson's ratio; φ_ε, scaling factor for strain; φ_σ, scaling factor for stress; φ_μ, scaling factor for the active coefficient of friction; φ_c, scaling factor for stiffness; φ_d, scaling factor for damping; and φ_f, scaling factor for frequency.

A. The Scaling Strategy of MMU

1. Principles

The important aspects of the behaviour that are being studied in a dynamic analysis are the displacements, velocities, and acceleration of the various bodies and the forces between these bodies and at the wheel–rail/roller interface.

As the most common measurements in dynamic studies are made in the form of time histories or frequency spectra the scaling factor for time and therefore frequency should be unity.

$$\varphi_t = 1 \tag{15.11}$$

The roller rig has been built to 1/5 full size to give suitable dimensions for construction and laboratory installation:

$$\varphi_l = 5 \tag{15.12}$$

Following the Equation 15.1 to Equation 15.6, gives rise to the following expressions:

$$\text{for displacement} \qquad \varphi_l = 5 \tag{15.13}$$

$$\text{for velocity} \qquad \varphi_v = 5 \tag{15.14}$$

$$\text{for acceleration} \qquad \varphi_a = 5 \tag{15.15}$$

and

$$\text{for frequency} \qquad \varphi_f = \frac{1}{\varphi_t} = 1 \tag{15.16}$$

which is convenient for comparison of these values.

2. Materials

Various options were available for the material used in the construction of the roller rig, but for ease of construction and to allow a reasonably practical wear life of the wheels and rollers it was convenient to use steel for these bodies. This is not a great disadvantage as the roller rig is not used to perform wear investigations, which would require correlation with the full scale case. The material properties are then similar on scale and full size: $\varphi_\rho = 1$ for density; $\varphi_E = 1$ for Young's modulus; $\varphi_\nu = 1$ for Poisson's ratio; $\varphi_\mu = 1$ for coefficient of friction.

Therefore the scaling factor for mass, considering Equation 3.7.8 is:

$$\varphi_m = 5^3 \tag{15.17}$$

and for rotational inertia, due to Equation 15.9:

$$\varphi_I = 5^5 \tag{15.18}$$

3. Equations of Motion

The equations of motion for a dynamic system govern the relationship between force and acceleration (and therefore velocity and displacement). In general terms, the basic equation is expressed in the form of a force balance and all force terms in the equation, for similarity, should equate to the force scaling term, φ_F.

$$m\ddot{x} + c\dot{x} + kx = F \tag{15.19}$$

and in the angular form:

$$I\ddot{\theta} + c_T\dot{\theta} + k_T\theta = T \tag{15.20}$$

where m is the mass; I is the moment of inertia; c, c_T are the damping coefficients; k, k_T are the stiffnesses; F is the applied force; and T is the applied torque.

Therefore, for the scale model, Equation 3.7.11 and Equation 3.7.12 become:

$$m\ddot{x}\left(\frac{\varphi_m\varphi_l}{\varphi_t^2}\right) + c\dot{x}\left(\frac{\varphi_c\varphi_l}{\varphi_t}\right) + kx(\varphi_k\varphi_l) = F(\varphi_F) \tag{15.21}$$

$$I\ddot{\theta}\left(\frac{\varphi_I}{\varphi_t^2}\right) + c_T\dot{\theta}\left(\frac{\varphi_{c_T}}{\varphi_t}\right) + k_T\theta\left(\frac{\varphi_{k_T}}{\varphi_t}\right) = T(\varphi_T) \tag{15.22}$$

For the translational case, from Equation 3.7.13 and for similarity:

$$\left(\frac{\varphi_m\varphi_l}{\varphi_t^2}\right) = \left(\frac{\varphi_c\varphi_l}{\varphi_t}\right) = (\varphi_k\varphi_l) = (\varphi_F) \tag{15.23}$$

therefore using the previously derived scaling factors for, φ_l, φ_m, and φ_t:

$$\varphi_l^4 = \varphi_c\varphi_l = \varphi_k\varphi_l = \varphi_F \tag{15.24}$$

giving $\varphi_c = 5^3$ for the translational damping coefficient; $\varphi_k = 5^3$ for the translational stiffness constant; and $\varphi_F = 5^4$ for the applied force.

For the rotational case, from Equation 3.7.14 and for similarity:

$$\left(\frac{\varphi_I}{\varphi_t^2}\right) = \left(\frac{\varphi_{c_T}}{\varphi_t}\right) = \left(\frac{\varphi_{k_T}}{\varphi_t}\right) = (\varphi_T) \tag{15.25}$$

therefore using the previously derived scaling factors for, φ_I and φ_t:

$$\varphi_I = \varphi_{c_T} = \varphi_{k_T} \tag{15.26}$$

giving $\varphi_{c_T} = 5^5$ for the rotational damping coefficient; $\varphi_{k_T} = 5^5$ for the rotational stiffness constant; and $\varphi_T = 5^5$ for the applied torque.

The above terms of power x^5 are validated by considering that a translational spring of stiffness k will give a torsional stiffness of kl^2, hence giving rise to the power raise of two. Therefore similarity is maintained in all equations with forces scaling at 5^4 and torques scaling at 5^5.

4. Scaling and Wheel–Rail/Roller Forces

A complete study of the scaling methodology must also include the effect of scaling on the equations governing the wheel–rail/roller interaction. A complete derivation of the equations of motion for a railway vehicle is not required for this study as the wheel–rail forces act through the

wheelset alone. Therefore the equations of motion for a single bogie vehicle, which includes some simple suspension forces is sufficient. The creep forces are derived from Kalker's linear theory.

The lateral equation of motion for a simple linear vehicle model can be represented by the following expressions:

$$m\ddot{y}_w + 2f_{22}\left(\frac{\dot{y}_w}{v} - \psi_w\right) + 2f_{23}\left(\frac{\dot{\psi}_w}{v} - \frac{\varepsilon_0}{l_0 r_0}\right) + \frac{w\varepsilon_0 y_w}{l_0} + \mathrm{d}_y(\dot{y}_w - \dot{y}_b - a\dot{\psi}_b + h\dot{\theta}_b)$$
$$+ c_y(y_w - y_b - a\psi_b + h\theta_b) \tag{15.27}$$

and the terms influencing the yaw of the wheelset:

$$I_z\ddot{\psi}_w + 2f_{11}\left(\frac{l_0^2\dot{\psi}_w}{v} + \frac{l_0\lambda y_w}{r_0}\right) - 2f_{23}\left(\frac{\dot{y}_w}{v} - \psi_w\right) + 2f_{33}\left(\frac{\dot{\psi}_w}{v}\right) + c_\psi(\psi_w - \psi_b) \tag{15.28}$$

where m is the wheelset mass; y_w is the wheelset lateral displacement; y_b is the bogie lateral displacement; ψ_w is the wheelset yaw angle; ψ_b is the bogie yaw angle; θ_b is the bogie roll angle; d_y is the wheelset–bogie lateral damping (per wheelset); c_y is the wheelset–bogie lateral stiffness (per wheelset); c_ψ is the wheelset–bogie yaw stiffness (per wheelset); w is the axle load; λ is the effective conicity; l_0 is the semi gauge; a is half the bogie wheelbase; h is the height of the bogie centre of gravity above the wheelset axis; v is the forward speed of the vehicle; ε_0 is the rate of change of contact angle with y_w; r_0 is the rolling radius with the wheelset central; $f_{11}, f_{22}, f_{23}, f_{33}$ is Kalker's linear creep coefficients.

The equations governing the linear creep coefficients are:

$$\begin{aligned} f_{11} &= (ab)GC_{11} \quad f_{23} = (ab)^{3/2}GC_{23} \\ f_{22} &= (ab)GC_{22} \quad f_{33} = (ab)^2GC_{33} \end{aligned} \tag{15.29a}$$

where C_{ii} are Kalker's tabulated creep coefficients, G is the modulus of rigidity and a and b are the contact patch semi-axes.

Hertz theory governs the size of the contact patch and the relevant equations are also requoted as follows:

$$ab = mn[3\pi N(k_1 + k_2)/4k_3]^{\frac{2}{3}} \tag{15.29b}$$

where

$$k_1 = \frac{1 - \nu_R^2}{E_W} \qquad k_2 = \frac{1 - \nu_W^2}{E_R} \tag{15.29c}$$

and

$$k_3 = \frac{1}{2}\left[\frac{1}{r_1} + \frac{1}{r_1'} + \frac{1}{r_2} + \frac{1}{r_2'}\right] \tag{15.29d}$$

m and n are the elliptical contact constants, N is the normal force and the other parameters are as previously quoted.

The scaling factors can then be calculated:

$$\varphi_{k_1} = \varphi_{k_2} = \frac{1}{\varphi_E} = 1 \tag{15.30}$$

$$\varphi_{k_3} = \frac{1}{\varphi_l} = 5^{-1} \tag{15.31}$$

If the scaling factor for the normal force, φ_N is 5^4, as with all other forces then the scaling factor for the contact patch area, $\varphi_{(ab)}$ will be:

$$\varphi_{(ab)} = \left(\varphi_N \frac{\varphi_{k_1}}{\varphi_{k_3}}\right)^{\frac{2}{3}} = \left(\frac{\varphi_F}{\varphi_{k_3}}\right)^{\frac{2}{3}} = 5^{3.33} \tag{15.32}$$

From Equation 15.32 and Equation 15.29a, we can evaluate the scaling for the linear creep coefficients.

Therefore:

$$\varphi_{f_{11}} = \varphi_{f_{22}} = \varphi_E \varphi_{(ab)} = 5^{3.33} \tag{15.33}$$

$$\varphi_{f_{23}} = \varphi_E (\varphi_{(ab)})^{\frac{3}{2}} = 5^5 \tag{15.34}$$

$$\varphi_{f_{33}} = \varphi_E (\varphi_{(ab)})^2 = 5^{6.66} \tag{15.35}$$

With a normal force scaling factor of 5^4, we have a conflict with the vehicle weight scaling factor due to its mass multiplied by the acceleration due to gravity:

$$\varphi_w = \varphi_m \varphi_g = 5^3 \tag{15.36}$$

conflicting with

$$\varphi_N = 5^4$$

This conflict can be resolved by the use of support wires, with incorporated spring balances connected to each axle box, to remove the required amount of weight.

Considering the describing equations of motion given in Equation 15.27 and Equation 15.28, each term can be evaluated, including the scaling factors derived above for the linear creep coefficients, to check for the required scaling factor. A factor of 5^4 when considering a force term and 5^5 for a torque scaling factor. All terms agree with the scaling strategy and give perfect scaling apart from those listed below:

Force terms (required $\varphi_F = 5^4$)

$$2f_{22}\frac{\dot{y}_w}{v}\psi_w \qquad \text{gives a force scaling, } \varphi_F = 5^{3.33} \tag{15.37}$$

$$\frac{w\varepsilon_0 y_w}{l_0} \qquad \text{gravitational stiffness term gives, } \varphi_F = 5^3 \tag{15.38}$$

Torque terms (required $\varphi_T = 5^5$)

$$2f_{11}\left(\frac{l_0^2\dot{\psi}_w}{v} + \frac{l_0\lambda y_w}{r_0}\right) \text{gives a torque scaling, } \varphi_T = 5^{4.33} \tag{15.39}$$

$$2f_{33}\left(\frac{\dot{\psi}_w}{v}\right) \qquad \text{gives a torque scaling, } \varphi_T = 5^{5.66} \tag{15.40}$$

In practice, the value of f_{33} is much smaller than f_{11} and f_{22}, the gravitational stiffness term in Equation 15.38 is of the same order as the f_{33} terms during normal tread running of the wheel, therefore the major error sources with respect to scaling the simulated, scaled forces, with those of a full size vehicle are Equation 15.37 and Equation 15.39.

B. The Scaling Strategy of DLR

AS DLR was involved in the development of simulation software for railway vehicle dynamics, and in particular the nonlinear lateral dynamics which leads to the instability known as hunting. This instability is caused by a bifurcation in describing differential equations into a limit cycle and the strategy for the scaling of the roller rig was developed with respect to this.

Therefore, much like the MMU group, the starting point for the DLR scaling strategy focused on the nonlinear lateral behaviour of a single wheelset, suspended to an inertially moving body. An example equation is described in Ref. 17, for a wheelset with conical treads. The first component of this system of two coupled equations of motion is shown below:

$$\frac{m}{\chi}\ddot{y}_w = \frac{I_y \Gamma \nu}{\chi r_0}\dot{\psi}_w \frac{mgb_0}{\chi}\frac{c_y}{\chi}y_w + T_y + T_x\psi_w \tag{15.41}$$

The symbols used above denote the same quantities as described in the previous section, with the addition or replacement of the wheelset's rotational moment of inertia, I_y; the longitudinal creep force, T_x; the lateral creep force; T_y; $\Gamma = \delta_0/l_0 - r_0\delta_0$; the cone angle, δ_0; $\chi = \Gamma l_0/\delta_0$; $b_0 = 2\Gamma + \Gamma^2(R_R + r_0)$; the transverse radius of the rail head, R_R.

Multiplying the scaleable parameters and variables in Equation 15.41 with the previously defined scaling factors and re-arranging:

$$\frac{m}{\chi}\ddot{y}_w = \frac{I_y \Gamma \nu}{\chi r_0}\dot{\psi}_w \frac{mgb_0}{\chi} y_w \frac{\varphi_t^2}{\varphi_l}\frac{c_y}{\chi} y_w \frac{\varphi_c \varphi_t^2}{\varphi_m} + (T_y + T_x\psi_w)\frac{\varphi_T \varphi_t^2}{\varphi_m \varphi_l} \tag{15.42}$$

Dynamically, the scale wheelset behaves similarly to the full scale, if Equation 15.41 and Equation 15.42 coincide. This requires that the following conditions hold:

$$\begin{aligned}
\frac{\varphi_t^2}{\varphi_l} &= 1 \Rightarrow \varphi_v = \sqrt{\varphi_l} && \text{velocity scaling} \\
\frac{\varphi_c \varphi_t^2}{\varphi_m} &= 1 \Rightarrow \varphi_c = \varphi_\rho \varphi_l^2 && \text{stiffness scaling} \\
\frac{\varphi_T \varphi_t^2}{\varphi_m \varphi_l} &= 1 \Rightarrow \varphi_T = \varphi_\rho \varphi_l^3 && \text{creep force scaling}
\end{aligned} \tag{15.43}$$

It can be seen that for similarity to be maintained the scaling factors for the Equation 15.43 above cannot be freely chosen and are a function of the principle scaling terms derived in Section IV.A. This result is identical to that found by Matsudaira et al.,[19] from investigations carried out in 1968 at the RTRI of the Japanese railways. From the constraint equations (a relationship between the normal forces, gyroscopic, gravitational, applied, and creep forces, see Ref. 8), together with the scaling method described above, the scaling factors for the constraint forces, the mass and creep

forces can be derived:

$$\varphi_N = \varphi_m = \varphi_T = \varphi_P \varphi_l^3 \tag{15.44}$$

This results in a scale factor for friction coefficient μ:

$$\varphi_\mu = 1$$

Assuming that Kalker's nonlinear theory is used for calculation of the contact forces, then similarity is required for the dimensions of the contact ellipse, if the calculated Kalker creep coefficients, and hence creep forces are to be correct. This requires that:

$$\varphi_E = \varphi_\nu = 1$$

If this condition is adhered to, then the scaling factor for density is derived as follows:

Kalker's theory requires that $\varphi_T = \varphi_{ab}$ and $\varphi_{ab} = (\varphi_N \varphi_l)^{2/3}$ and $\sqrt{\varphi_{ab}} = \varphi_e$ (the contact ellipse mean radius), then the scale of this radius becomes:

$$\varphi_e^3 = \varphi_N \varphi_l = \varphi_\rho \varphi_l^4 \tag{15.45}$$

Assuming geometric similarity for the contact ellipse, $\varphi_e = \varphi_l$, Equation 15.45, results in the definition of the density scaling factor:

$$\varphi_\rho = \frac{1}{\varphi_l}$$

This scaling factor, which would result in perfect scaling for the contact ellipse and Kalker coefficients, when considering the length scale factor $\varphi_l = 5$, requires a density which is very difficult to achieve. It was considered by DLR that exact scaling of the contact patch was only necessary at low levels of creepage and not so important during the analysis of limit cycles, where saturation of the creep forces occurs and the exact shape and size of the contact patch does not influence the creep forces (gross sliding within the contact region). Considering the above practical limitations, the density scaling factor was chosen as:

$$\varphi_\rho = \frac{1}{2}$$

which can be easily achieved and has proven through testing to give good experimental results.With

$$\varphi_l = 5$$

and considering the above-mentioned limitation with respect to density, the other scaling factors can be determined as follows:

$$\varphi_v = \sqrt{\varphi_l} = \sqrt{5} \qquad \text{velocity}$$

$$\varphi_t = \frac{\varphi_l}{\varphi_v} = \sqrt{5} \qquad \text{time}$$

$$\varphi_a = \frac{\varphi_l}{\varphi_t^2} = 1 \qquad \text{acceleration}$$

$$\varphi_m = \varphi_T = \varphi_N = \varphi_F = \varphi_\rho \varphi_l^3 = 62.5 \qquad \text{mass and force}$$

$$\varphi_I = \varphi_\rho \varphi_l^5 = 1562.5 \qquad \text{moment of inertia}$$

$$\varphi_c = \varphi_\rho \varphi_l^2 = 12.5 \qquad \text{spring stiffness}$$

$$\varphi_d = \frac{\varphi_\rho \varphi_l^3}{\varphi_v} = \varphi_\rho \varphi_l^{5/2} = 27.95 \qquad \text{viscous damping}$$

$$\varphi_f = \frac{1}{\varphi_t} = \frac{1}{\sqrt{5}} \qquad \text{frequency}$$

$$\varphi_\mu = \frac{\varphi_T}{\varphi_N} = 1 \qquad \text{coefficient of friction}$$

$$\varphi_e = (\varphi_N \varphi_l)^{1/3} = 6.79 \qquad \text{contact ellipse}$$

Table 15.1 below shows some typical parameters for a generic test vehicle using the DLR scaling strategy.

C. The Scaling Strategy of INRETS

Within the INRETS institution the main area of research focus was the experimental validation of Kalker's creep coefficients. The vehicle scale at INRETS is large compared to other rigs at 1:4, coupled with the very large roller diameter means the rig is suitable for the analysis of wheel/rail

TABLE 15.1
Generic Test Vehicle Parameters

Parameter	Full-Size	1/5 Scale
	Bogie	
Bogie frame mass	487.50 kg	7.8 kg
Wheel mass	281.25 kg	4.5 kg
Axle mass	275.00 kg	4.4 kg
Bogie roll inertia	218.75 kg/m^2	0.14 kg/m^2
Bogie pitch inertia	103.13 kg/m^2	0.066 kg/m^2
Bogie yaw inertia	192.19 kg/m^2	0.123 kg/m^2
Wheel rotational inertial	51.56 kg/m^2	0.033 kg/m^2
Axle rotational inertia	3.13 kg/m^2	0.002 kg/m^2
	Vehicle Body	
Body mass	2037.50 kg	32.6 kg
Body roll inertia	1403.13 kg/m^2	0.898 kg/m^2
Body pitch inertia	1339.06 kg/m^2	0.857 kg/m^2
Body yaw inertia	2342.19 kg/m^2	1.499 kg/m^2
	Wheel Dimensions	
Wheel diameter	1.0 m	0.2 m
Gauge	1.435 m	0.287 m
	Primary Suspension	
Longitudinal stiffness	8.30×10^5 N/m	6.64×10^4 N/m
Lateral stiffness	8.30×10^5 N/m	6.64×10^4 N/m
Vertical stiffness	5.90×10^7 N/m	4.73×10^6 N/m
Normal force	11,496 N	183.94 N

contact. The validation of Kalker's theory requires exact representation of the contact patch and its elasticity, to allow accurate measurement of the quasistatic creepage and creep force relationships. Therefore the basis of the scaling strategy was obtained by adopting a stress scaling factor of

$$\varphi_\sigma = \frac{\varphi_F}{\varphi_l^2} = 1.$$

This means that the stresses in the scale and full scale test vehicle are the same. In addition to the advantages in investigating Kalker's theory, this stress scale factor results in a spring scaling factor which is proportional to the length factor. This helps in the design of suspension components as size and internal stresses are the same as the full scale:

$$\varphi_c = \frac{\varphi_F}{\varphi_l} = \varphi_l = 4 \tag{15.46}$$

When similarity of elastic forces, together with similarity of gravitational forces is required, then the following is true:

$$\varphi_c \varphi_l = \varphi_m \varphi_g \tag{15.47}$$

where φ_g is the scaling factor for gravity. Equation 15.46 shows that for the requirement of a valid frequency scaling factor, then the frequency of a mass spring system should be the same as that of an equivalent gravitational oscillator, such as a pendulum, this condition yields that:

$$\varphi_w^2 = \frac{\varphi_c}{\varphi_m} = \frac{\varphi_g}{\varphi_l} \tag{15.47a}$$

Assuming the density scaling factor $\varphi_\rho = 1$, Equation 15.47 leads to a gravity scaling factor of

$$\varphi_g = \frac{1}{\varphi_l} = \frac{g_1}{g_0} \tag{15.48}$$

The above equation essentially results in a different scaling factor for forces generated through gravitation and those generated from inertia and in a similar way to the MMU strategy, this can be achieved by application of external forces, which adds to the effective weight, without increasing mass. Considering Equation 15.42, this results in a scaling factor for weight of

$$\varphi_w = \frac{m_1 g_1}{m_0 g_0 \varphi_l} \Rightarrow \varphi_w = \varphi_l^2 = 16 \tag{15.49}$$

whereas the inertial force scaling factor with $\varphi_g = 1$

$$\varphi_m \varphi_g = \varphi_\rho \varphi_l^3 \Rightarrow \varphi_w = \varphi_l^3 = 64 \tag{15.50}$$

Using this strategy, increasing the weight through an external force which does not change the mass of the body allows the derivation of scaling factors for velocity, time, and acceleration to be formed from the frequency Equation 15.5 and Equation 15.6.

$$\left(\frac{\varphi_v}{\varphi_l}\right) = \frac{\varphi_c}{\varphi_m} \Rightarrow \varphi_v = 1$$

$$\varphi_t = \varphi_l$$

$$\varphi_a = \varphi_l \tag{15.51}$$

TABLE 15.2
Comparison of Scaling Strategies

Scaling	MMU	DLR	INRETS
	Geometry		
Length	5	5	4
Cross-section	25	25	16
Volume	125	125	64
	Material		
Density	1	0.5	1
Mass	125	62.5	64
Inertia	3125	1562.5	1024
Elasticity	G,E,cij	approximate	G,E,cij
	Parameters		
Time	1	$\sqrt{5}$	4
Frequency	1	$1/\sqrt{5}$	1/4
Velocity	5	$\sqrt{5}$	1
Acceleration	5	1	4
Stress	25	5	1
Strain	5	5	1
Stiffness	125	12.5	4
	Forces		
Inertial forces	625	62.5	16
Gravitational forces	Reduced by 1/5	62.5	Multiply by 4
Spring forces	Modified	62.5	Scaled
Viscous damping forces	Modified	62.5	Not considered

The above scaling strategy results in similarity of vertical dynamics, together with elastic contact, normal and tangential stresses, which in turn allows the lateral dynamics to be accurately represented.

D. Tabular Comparison of Scaling Strategies

To summarise the strategies discussed in the above section, the scaling parameters have been listed in Table 15.2.

V. SCALING ERRORS

As discussed, a scaling strategy is selected based on the type of analysis work to be carried out on the rig, this type specific selection of the strategy has to be performed as perfect scaling cannot be achieved. The example below, using the scaling strategy of the Manchester Metropolitan University, illustrates the level of error which can be encountered.

The errors caused by the scaling of a vehicle can be expressed by the following equations, which have been reproduced from Section IV.A.4 for convenience:

Force terms (required $\varphi_F = 5^4$)

$$2f_{22}\left(\frac{\dot{y}_w}{v} - \psi_w\right) \qquad \text{gives a force scaling, } \varphi_F = 5^{3.33} \tag{15.52}$$

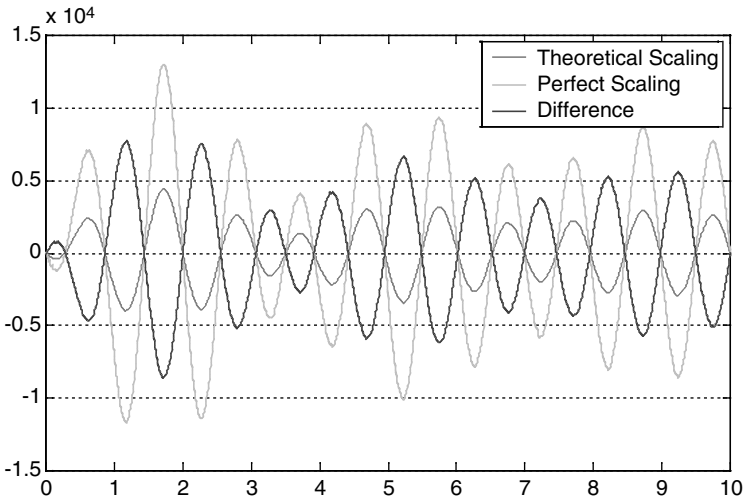

FIGURE 15.6 Lateral force scaling error.

Torque terms (required $\varphi_T = 5^5$)

$$2f_{11}\left(\frac{l_0^2\dot{\psi}_w}{v} + \frac{l_0\lambda y_w}{r_0}\right) \qquad \text{gives a torque scaling, } \varphi_T = 5^{4.33} \tag{15.53}$$

$$2f_{33}\left(\frac{\dot{\psi}_w}{v}\right) \qquad \text{gives a torque scaling, } \varphi_T = 5^{5.66} \tag{15.54}$$

The expected level of error from the terms highlighted above can be quantified by performing an analysis of a two degree of freedom wheelset model. The results of the theoretical scaling strategy are plotted against the same model but simulated with a perfect scaling strategy.

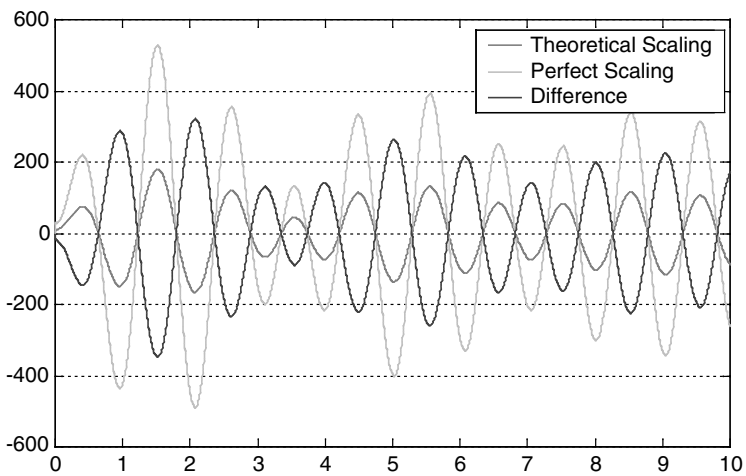

FIGURE 15.7 Wheelset torque scaling error.

The plots shown in Figure 15.6 and Figure 15.7 quantify the errors due to the scaling factors derived in Equation 15.52 to Equation 15.54. The plots were produced with a two degree of freedom model, excited with a sinusoidal disturbance, with an amplitude of 0.5 mm and a frequency of 2π radians per second. The forward speed of the vehicle was a 1/5 scale speed of 2 or 10 m/sec at full scale. The results have been scaled from the 1/5 scale values of the roller rig, to the full scale, all other terms achieve perfect scaling.

Although perfect scaling has not been achieved for these terms, experimental testing has shown that the adopted scaling strategy gives good agreement with the full scale, particularly when considering stability. For the purpose of relative studies between vehicles on the roller rig, the error in creep forces illustrated in Figure 15.6 and Figure 15.7 are not of great significance but modifications to the scaling method, to reduce this error, may be required if absolute values between scaled and full-size creep forces, were required.

VI. CONCLUSIONS

This chapter has discussed the history and application of scaled roller rigs, their uses and has described the construction and operation of three scaled roller rigs from Manchester Metropolitan University, INRETS, and DLR. The three scaling strategies of the above institutions have been described in detail and the differences tabulated.

It is important when designing a new roller rig to first consider the primary use of the rig as this will help form the basis of the scaling strategy. The scaling strategy is the most important aspect of the rig development as it will ensure that the measured parameters are correctly related and obey laws of similarity.

In summary, the scaling strategy of the rig at MMU, Manchester, was developed using a comparison of the linearised differential equations for the scale and full size, the main purpose of the rig being the study of vehicle stability and general dynamic behaviour. Frequency was preserved at 1:1 for this type of analysis. The scaling method for the rig at DLR, Oberpfaffenhofen, was derived from a study of the full set of nonlinear equations of motion to give precise results for study of limit cycle behaviour and early validation of the dynamic multibody simulation software, SIMPACK. The large single wheel rig at INRETS in Grenoble, allows suspension parameters to be evaluated and the almost exact treatment of the contact conditions, allowed by the very large radius of roller. The rig has been used extensively for the validation of Kalker's theory and development of in-house contact mechanics software.

As has been detailed in Chapter 14, there are errors inherent in roller rig testing and these of course apply to scaled rigs. It must be realised that scaled rigs also have additional errors introduced by the scaling strategy, as perfect scaling for all parameters cannot be achieved. An example of possible scaling errors is given and the errors analysed using a typical two degree of freedom wheelset model. This analysis illustrates the importance of selecting a scaling strategy which suits the desired use of the rig.

It is sensible with a scaled roller to use the largest possible roller diameter irrespective of the scale defined for the bogie, as this will preserve the contact conditions with respect to running on conventional track. Results have been presented in the previous chapter as to the influence of roller diameter on various parameters, and these should be considered at the design stage of a scaled rig.

ACKNOWLEDGMENTS

The author wishes to acknowledge the contribution of Alfred Jaschinski and Hugues Chollet, whose work has been presented, in part, under information submitted regarding the DLR and INRETS scaled roller rigs, respectively.[20]

REFERENCES

1. Reynolds, O., An experimental investigation of the circumstances which determine whether the motion of water shall be direct or sinous, and the law of resistance in parallel channels, *Phil. Trans. R. Soc.*, 174, 935–953, 1883.
2. Reynolds, O., On the dynamical theory of incompressible viscous fluids and the determination of the criterion, *Phil. Trans. R. Soc.*, 186, 123–164, 1895.
3. Sweet, L. M., Sivak, J. A., and Putman, W. F., Non-linear wheelset forces in flange contact, part I: steady state analysis and numerical results, part 2 measurement using dynamically scaled models, *J. Dyn. Syst., Meas. Control*, 101, 238–255, 1979.
4. Sweet, L. M., Karmel, A., and Fairley, S. R., Derailment mechanics and safety criteria for complete railway vehicle trucks, In *The Dynamics of Vehicles on Roads and Tracks*, *Proceedings of Seventh IAVSD Symposium, Cambridge, UK, September 1981*, Wickens, A., Ed., Swets & Zeitlinger, Lisse, 1982.
5. Cox, M. and Nicolin, H., Untersuchung des Schwingungsverhaltens von Schienenfahrzeugen mit Hilfe des Modellprüfstands am Institut fur FSrdertechnik und Schienenfahrzeuge der RWTH Aachen, *Leichtbau der Verkehrsfahrzeuge*, 23(4), 91–95, 1979.
6. Jochim, M., Konstruktion eines Versuchsdrehgestells. Term study, Lehrstuhl B fur Mechanik, Tu-München and DLR, Oberpfaffenhofen, 1984.
7. Jochim, M., Analyse der Dynamik eines Schienenfahrzeuges. Diploma thesis, Lehrstuhl B fur Mechanik, TU-München and DLR, Oberpfaffenhofen, 1987.
8. Jaschinski, A., On the application of similarity laws to a scaled railway bogie model. Dissertation, TU-Delft, 1990 and DLR-FB 90-06, Oberpfaffenhofen, 1990.
9. Heliot, C., Small-scale test method for railway dynamics, In *The Dynamics of Vehicles on Roads and Tracks*, *Proceedings of Ninth IAVSD Symposium, Linkoping, Sweden, June 1985*, Nordstrom, C., Ed., Swets & Zeitlinger, Lisse, 1986.
10. Iwnicki, S. D. and Shen, Z. Y., *Collaborative Railway Roller Rig Project*, *Proceedings of SEFI World Conference on Engineering Education,* Portsmouth, September, 1992.
11. Iwnicki, S. D. and Wickens, A. H., Validation of a MATLAB railway vehicle simulation using a scale roller rig, *Veh. Syst. Dyn.*, 30(3), 257–270, 1998.
12. Allen, P. D., Error Quantification of a Scaled Roller Rig, Doctoral thesis, Manchester Metropolitan University, 2001.
13. Jaschinski, A. and Netter, H., Non-linear dynamical investigations by using simplified wheelset models, In *The Dynamics of Vehicles on Roads and Tracks*, *Proceedings of 12th IAVSD Symposium, Lyon, France, August 26–30, 1991*, Sauvage, G., Ed., Swets & Zeitlinger, Amsterdam/Lisse, 1992.
14. Meinke, P. and Mauer, L., Koppelrahmen-Laufdrehgestell fur ICE-Mittelwagen, VDI-Berichte, No. 634, pp. 203–219, 1987.
15. Chollet, H., Essais en similitude a 1'echelle 1/4 de bogies de wagons de la famille Y25 INRETS-Report No. 78, 1988.
16. Mauer, L. and Meinke, P., Requirements of future high-speed running gears. RTR Special Railway Technical Review, September 1993.
17. Jaschinski, A., Grupp, F., and Netter, H., Parameter identification and experimental investigations of unconventional railway wheelset designs on a scaled roller rig, In *The Dynamics of Vehicles on Roads and Tracks*, *Proceedings of 14th IAVSD Symposium, Ann Arbor, Michigan, 1995*, Segel, L., Ed., Swets & Zeitlinger, Lisse, 1996.
18. Wickens, A. H., The dynamics of railway vehicles on straight track: fundamental considerations of lateral stability, *Proc. I. Mech. Eng.*, 180, 29–44, 1965.
19. Matsudaira, T., Matsui, N., Arai, S., and Yokose, K., Problems on hunting of railway vehicle on test stand, *Trans. A.S.M.E.J. Eng. Ind.*, 91(3), 879–885, 1969, ser. B.
20. Jaschinski, A., Chollet, H., Iwnicki, S. D., Wickens, A. H., and Von Würzen, J., The application of roller rigs to railway vehicle dynamics, *Veh. Syst. Dyn.*, 31, 345–392, 1999.
21. Illingworth, R., Railway wheelset lateral excitation by track irregularities, In *The Dynamics of Vehicles on Roads and Tracks*, *Proceedings of 5th VSD-2nd IUTAM Symposium*, *Vienna*, *Austria*, *September 19–23*, *1977*, Slibar, A., Ed., Swets & Zeitlinger, pp. 450–458, 1978.